

The Structure and Electrical Properties of Nb₈PtSe₂₀

STEVEN A. SUNSHINE AND JAMES A. IBERS

Department of Chemistry, Northwestern University, Evanston, Illinois 60201

Received September 15, 1986; in revised form December 29, 1986

The new layered ternary chalcogenide Nb₈PtSe₂₀ has been synthesized and structurally characterized. This compound crystallizes in the monoclinic system in space group C_{2h}^3-C2/m with cell dimensions $a = 20.096(12)$, $b = 3.433(2)$, $c = 19.289(11)$ Å, and $\beta = 107.1(5)^\circ$. This structure contains four unique Nb atoms, two in trigonal prismatic environments, one in a monocapped trigonal prismatic site, and one in a bicapped trigonal prism of Se atoms. The bicapped trigonal prism contains an Se-Se bond ($d = 2.36(2)$ Å). The Pt atoms exhibit square-planar coordination. Electrical conductivity measurements over the temperature range 110-300 K indicate that this material is a metal ($\sigma_{RT} = 1.5 \times 10^3 \Omega^{-1} \text{cm}^{-1}$). © 1987 Academic Press, Inc.

Introduction

The early transition-metal trichalcogenides (MQ_3 , $M = \text{Group IV, V}$; $Q = \text{S, Se}$) have been extensively studied because of their interesting structural chemistry (1-6) and fascinating physical properties (5-11). The trichalcogenides are characterized by metal-centered bicapped trigonal prisms of Q atoms. The trigonal prisms contain $Q-Q$ bonds that vary in length depending on the metal atom. Despite the great interest in the trichalcogenides, only a few ternary compounds exist that contain structural units similar to those found in the MQ_3 structures (12, 13). One of these, FeNb₃Se₁₀, exhibits charge density wave phenomena similar to those of NbSe₃ (14, 15). Investigation of the Nb-Pt-Se system for further examples of this chemistry has led to the compound Nb₈PtSe₂₀. This compound contains the same structural unit that is found in NbSe₃ and possesses an Se-Se bond ($d = 2.36(2)$ Å).

Experimental

The compound Nb₈PtSe₂₀ was prepared by heating Nb powder (99.8%, Alfa), Pt powder (99.9%, Johnson-Matthey), and Se powder (99.999%, Atomergic) in a 2:1:7 ratio in an evacuated ($\sim 10^{-5}$ torr) silica tube for 150 hr at 900 K. Thin black needles formed at the charge end of the tube. The presence of all three elements was confirmed by a microprobe analysis. Calcd. for Nb₈PtSe₂₀: Nb, 29.5; Pt, 7.8; Se, 62.7%; found from conventional chemical analysis: Nb, 28.4; Pt, 6.2; Se, 63.0%.

Four-probe electrical conductivity measurements were made along the needle axis, b , of a single crystal with the use of previously described procedures (16).

On the basis of Weissenberg photographs, crystals of Nb₈PtSe₂₀ were assigned to the Laue group $2/m$. The systematic extinction, hkl , $h + k = 2n + 1$, is consistent with the space groups C_{2h}^3-C2/m , C_s^3-Cm , and C_2^3-C2 . After an absorption

correction was applied, the reflections equivalent in space groups $C2/m$, Cm , and $C2$ were averaged to yield the residuals $R = 0.17$, 0.16 , and 0.16 , respectively. As the averaging in the three possible space groups is similar, we favor the centrosymmetric group $C2/m$.

Intensity data were collected on a Picker FACS-1 diffractometer with the ω scan technique and graphite-monochromated $\text{MoK}\alpha$ radiation (17). The crystals grow as needles that bend and fray easily; crystal quality is poor. A large scan range (2.6° in ω) was needed owing to considerable peak broadening. Six standard reflections measured every 100 reflections showed no significant variation in intensity. Crystal data and data collection parameters are given in Table I.

All calculations were performed on a Harris 1000 computer with programs standard in this laboratory (17). The structure was solved by direct methods. An E-map revealed the positions of all atoms except Nb(4), Se(4), and Se(10); these were located in subsequent electron density maps. The final cycle of refinement was performed on F_o^2 and included isotropic thermal parameters for all atoms. The final agreement indices for data with $F_o^2 > 0$ are $R = 0.241$ and $R_w = 0.214$. The value of the conventional R index for 304 reflections having $F_o^2 > 3\sigma(F_o^2)$ is 0.096. The final difference electron density map contains no feature greater than 8% of the height of a Pt atom. Analysis of F_o^2 vs F_c^2 as a function of F_o^2 , setting angles, and Miller indices reveals no unusual trends.

Final atomic parameters and isotropic thermal parameters appear in Table II. Structure amplitudes are presented in Table S-I.¹

¹ See NAPS document No. 04465 for 6 pages of supplementary material. Order from ASIS/NAPS. Microfiche Publications, P.O. Box 3513, Grand Central Station, New York, NY 10163. Remit in advance

TABLE I
CRYSTAL DATA AND INTENSITY CALCULATION
PARAMETERS FOR $\text{Nb}_8\text{PtSe}_{20}$

Formula	$\text{Nb}_8\text{PtSe}_{20}$
Formula weight (amu)	2517.5
Space group	C_{2h}^2-C2/m
a (\AA) ^a	20.096(12)
b (\AA)	3.433(2)
c (\AA)	19.289(11)
β (deg)	107.1(5)
V (\AA^3)	1272.2
Z	2
T of data collection (K) ^b	120
Density (calc.) (g cm^{-3})	6.57
Crystal volume (mm^3)	2.19×10^{-5}
Crystal shape	Flattened needle bound by {101}, {010}, {101}
Radiation	Graphite monochromated $\text{MoK}\alpha$ ($\lambda(K\alpha_1) = 0.7093 \text{ \AA}$)
Linear abs. coeff. (cm^{-1})	372
Transmission coefficients ^c	0.646–0.856
Detector aperture (mm)	4 wide by 4.5 high, 32 cm from crystal
Takeoff angle (deg)	2.5
Scan speed (deg min^{-1})	1.0
Scan range (deg ω)	2.6
$\lambda^{-1} \sin \theta$, limits (\AA^{-1})	0.0512–0.5958 $2^\circ \leq 2\theta (\text{MoK}\alpha_1) \leq 50^\circ$
Background counts ^d	10 sec at each end of scan with rescan option
Data collected	$\pm h \pm k \pm l$ $2^\circ < 2\theta \leq 30^\circ$ $hk \pm l$ $30^\circ < 2\theta \leq 50^\circ$
ρ factor	0.04
No. of unique data	1321
No. of unique data with $F_o^2 > 0$	1014
No. of unique data with $F_o^2 > 3\sigma(F_o^2)$	304
No. of variables	44
R (F^2) for $F_o^2 > 0$	0.241
R_w (F^2) for $F_o^2 > 0$	0.214
R (on F for $F_o^2 > 3\sigma(F_o^2)$)	0.096
Error in observation of unit wt. (e^2)	1.03

^a Refinement of the cell restricted α and γ to 90° .

^b The low-temperature system is based on a design by J. C. Huffman, Ph.D. thesis, Indiana University, 1974.

^c The analytical method was used for the absorption correction (J. de Meulenaer and H. Tompa, *Acta Crystallogr.* **19**, 1014 (1965)).

^d The diffractometer was operated under the Vanderbilt disk-oriented system.

In the above calculations the idealized composition $\text{Nb}_8\text{PtSe}_{20}$ was used. Although the chemical analysis is slightly low in Pt,

\$4.00 for microfiche copy or for photocopy, \$7.75. Foreign orders add \$4.50 for postage and handling, \$1.50 for postage of any microfiche orders.

TABLE II
POSITIONAL PARAMETERS AND ISOTROPIC THERMAL PARAMETERS FOR Nb₈PtSe₂₀

Atom	Wyckoff notation	Site symmetry	x	y	z	B _{iso} (Å ²)
Pt	2b	2/m	1/2	0	0	0.7(1)
Nb(1)	4i	m	0.07673(57)	0	-0.09026(58)	0.8(2)
Nb(2)	4i	m	0.33125(53)	0	0.18880(55)	0.6(2)
Nb(3)	4i	m	0.26872(48)	0	-0.27911(51)	0.1(2)
Nb(4)	4i	m	0.15013(50)	0	0.44207(53)	0.6(2)
Se(1)	4i	m	0.13911(53)	0	0.29887(55)	0.0(2)
Se(2)	4i	m	0.37680(56)	0	-0.01374(58)	0.6(2)
Se(3)	4i	m	0.19904(54)	0	0.17342(56)	0.1(2)
Se(4)	4i	m	0.45056(54)	0	-0.38606(57)	0.5(2)
Se(5)	4i	m	0.25380(55)	0	-0.42635(57)	0.3(2)
Se(6)	4i	m	0.33350(58)	0	0.32493(60)	0.8(2)
Se(7)	4i	m	0.47504(55)	0	-0.13218(57)	0.5(2)
Se(8)	4i	m	0.20677(62)	0	-0.08412(64)	1.0(2)
Se(9)	4i	m	0.06857(57)	0	-0.22844(59)	0.6(2)
Se(10)	4i	m	0.40488(55)	0	0.48656(57)	0.7(2)

this could arise from lack of homogeneity of the bulk sample. Owing to the poor quality of the X-ray data, no attempt was made to establish the composition of the X-ray crystal through refinement of occupancies. But the thermal parameters of Table II suggest that the idealized composition is a reasonable one.

Discussion

A drawing of the structure of Nb₈PtSe₂₀ with the labeling scheme is given in Fig. 1. Selected bond distances and angles are given in Table III. The structure is a new laminar type with the layers extending parallel to (201). A view of an individual layer as viewed orthogonal to (201) is provided in Fig. 2. Each chain in this structure contains eight Nb atoms between two Pt atoms in square-planar sites. One-half of the chain is related to the second half by an inversion center. The four unique Nb atoms possess a variety of coordination geometries; trigonal prismatic (Nb(1), Nb(2)), monocapped tri-

gonal prismatic (Nb(3)), and bicapped trigonal prismatic (Nb(4)). The bicapped trigonal prism of Se atoms contains an Se-Se bond.

These geometries around the Pt and Nb atoms have been seen in other structures. The average Pt-Se distance of 2.43(1) Å

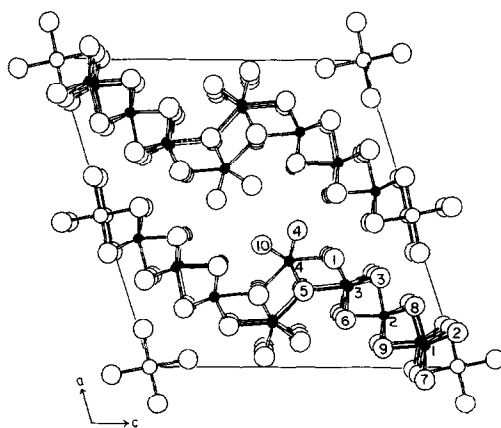


FIG. 1. View of the structure of Nb₈PtSe₂₀ along [010] with the labeling scheme. Here and in Fig. 2 small solid circles are Nb atoms, small open circles are Pt atoms, and large open circles are Se atoms.

TABLE III
SELECTED BOND DISTANCES (Å) AND ANGLES (deg) FOR Nb₈PtSe₂₀

Pt–2Se(2)	2.41(1)	Se(4)–Se(10)	2.36(2)
Pt–2Se(7)	2.45(1)		
Pt–4Nb(1)	3.152(8)	Se(2)–Pt–Se(7)	89.8(3)
Pt–2Pt	3.433(2)		
Nb(1)–1Se(8)	2.58(2)	Se(8)–Nb(1)–Se(2)	80.5(4)
Nb(1)–2Se(2)	2.60(1)	Se(8)–Nb(1)–Se(9)	78.9(5)
Nb(1)–2Se(7)	2.61(1)	Se(2)–Nb(1)–Se(2)	82.8(5)
Nb(1)–1Se(9)	2.62(2)	Se(2)–Nb(1)–Se(7)	82.9(3)
Nb(1)–2Nb(1)	3.433(2)	Se(7)–Nb(1)–Se(7)	82.3(4)
Nb(1)–2Nb(2)	3.47(1)	Se(7)–Nb(1)–Se(9)	82.9(4)
Nb(2)–2Se(9)	2.58(1)	Se(3)–Nb(2)–Se(9)	136.0(3)
Nb(2)–1Se(3)	2.59(1)	Se(3)–Nb(2)–Se(6)	80.2(4)
Nb(2)–2Se(8)	2.59(1)	Se(9)–Nb(2)–Se(9)	83.2(4)
Nb(2)–1Se(6)	2.61(2)	Se(9)–Nb(2)–Se(8)	79.4(3)
Nb(2)–2Nb(2)	3.433(2)	Se(8)–Nb(2)–Se(8)	83.1(5)
Nb(2)–1Nb(3)	3.47(1)	Se(8)–Nb(2)–Se(6)	134.3(3)
Nb(3)–2Se(3)	2.60(1)	Se(3)–Nb(3)–Se(3)	82.7(4)
Nb(3)–2Se(6)	2.62(1)	Se(3)–Nb(3)–Se(6)	79.8(3)
Nb(3)–2Se(1)	2.63(1)	Se(3)–Nb(3)–Se(1)	70.1(3)
Nb(3)–1Se(5)	2.77(1)	Se(6)–Nb(3)–Se(1)	92.2(3)
Nb(3)–2Nb(3)	3.433(2)	Se(6)–Nb(3)–Se(5)	79.4(4)
Nb(4)–2Se(4)	2.63(1)	Se(1)–Nb(3)–Se(5)	73.8(3)
Nb(4)–2Se(10)	2.64(1)	Se(4)–Nb(4)–Se(4)	81.4(4)
Nb(4)–2Se(5)	2.67(1)	Se(4)–Nb(4)–Se(10)	53.1(3)
Nb(4)–1Se(1)	2.71(1)	Se(4)–Nb(4)–Se(5)	91.6(3)
Nb(4)–1Se(5)	2.77(1)	Se(10)–Nb(4)–Se(5)	94.0(2)
Nb(4)–2Nb(4)	3.433(2)	Se(1)–Nb(4)–Se(5)	138.5(5)

agrees well with the value of 2.429(6) Å found around the Pt atom with square-planar coordination in Ta₂Pt₃Se₈ (18). The Nb–Se distances for all three types of Nb coordination are in close accord with those found in similar structures (3, 19, 20). Trends such as the lengthened Nb–Se distances to the capping Se atoms (Nb(3)–Se(5) = 2.77(1) Å, Nb(4)–Se(1) = 2.71(1) Å, Nb(4)–Se(5) = 2.77(1) Å) are

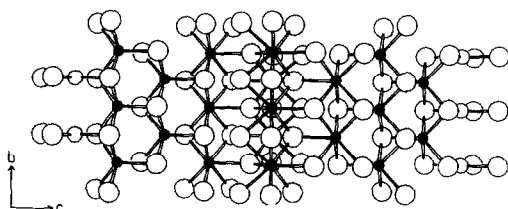


FIG. 2. Drawing of one layer of the Nb₈PtSe₂₀ structure as viewed orthogonal to (201).

also observed in Nb₃Pd_{0.72}Se₇ (20), Nb₂Pd_{0.71}Se₅ (19), and FeNb₃Se₁₀ (12). Furthermore, the Se–Se distance of 2.36(2) Å in the trigonal prism centered by Nb(4) is very similar to the value 2.374(4) Å found in NbSe₃ (3) and 2.348(1) Å found in FeNb₃Se₁₀ (12).

The structure of Nb₈PtSe₂₀ can be thought of as arising from the addition of two NbSe₃ units to the chains of the Nb₃Pd_{0.72}Se₇ structure (20). This suggests that the Pd analog of Nb₈PtSe₂₀ may also be stable. Because the Nb₃Pd_{0.72}Se₇ structure can be rationalized as the addition of NbSe₂ units to Nb₂Pd_{0.71}Se₅ (20), it may be possible to synthesize Nb₆PtSe₁₆, a structure where two NbSe₃ units have been added to the layers of Nb₂Pt_xSe₅, the hypothetical analog of Nb₂Pd_xSe₅.

A plot of the single-crystal conductivity

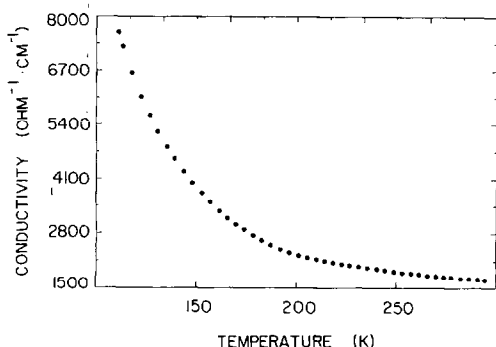


Fig. 3. Plot of the conductivity versus temperature for $\text{Nb}_8\text{PtSe}_{20}$.

data over the temperature range 110–300 K is given in Fig. 3. This material shows metallic behavior over this temperature range and does not exhibit phase transitions, although phase transitions are observed in NbSe_3 (10) and $\text{FeNb}_3\text{Se}_{10}$ (21). Electronic structure calculations on $\text{FeNb}_3\text{Se}_{10}$ (14) have shown that only one unpaired electron per unit cell is expected. For $\text{Nb}_8\text{PtSe}_{20}$ a simple valence argument suggests the formula $2\text{Nb}^{5+}6\text{Nb}^{4+}\text{Pt}^{2+}16\text{Se}^{2-}2(\text{Se}_2)^{2-}$ and predicts unpaired electrons on three different chains of Nb atoms.

The synthesis of $\text{Nb}_8\text{PtSe}_{20}$ clearly demonstrates the way in which additional one-dimensional chains can be added to low-dimensional structures (20). The incorporation of chains of NbSe_3 rather than NbSe_2 suggests that a variety of new compounds may be stable. More importantly, the presence of one-dimensional chains of NbSe_3 may account for the interesting physical properties observed in this material. Ideally this could lead to a set of compounds whose properties are altered by the addition of one-dimensional chains of NbSe_2 or NbSe_3 .

Acknowledgments

We are indebted to the Materials Research Center of Northwestern University for the use of the magnet, X-ray, and scanning electron microscope facilities,

supported in part under the NSF–MRL program (Grant DMR85-20280). We thank Johnson–Matthey, Inc. for the loan of Pt metal.

This research was supported by the U.S. National Science Foundation–Solid State Chemistry under Grant DMR83-15554.

References

1. J. RIJNSDORP AND F. JELLINEK, *J. Solid State Chem.* **25**, 325 (1978).
2. A. MEERSCHAUT, L. GUEMAS, AND J. ROUXEL, *J. Solid State Chem.* **36**, 118 (1981).
3. A. MEERSCHAUT AND J. ROUXEL, *J. Less-Common Met.* **39**, 197 (1975).
4. D. W. BULLETT, *J. Phys. C* **12**, 277 (1979).
5. J. A. WILSON, *Phys. Rev. B* **19**, 6456 (1979).
6. L. BRATTÅS AND A. KJEKSHUS, *Acta Chem. Scand.* **26**, 3441 (1972).
7. H. HARALDSEN, A. KJEKSHUS, E. RØST, AND A. STEFFENSEN, *Acta Chem. Scand.* **17**, 1283 (1963).
8. E. BJERKELUND, J. H. FERMOR, AND A. KJEKSHUS, *Acta Chem. Scand.* **20**, 1836 (1966).
9. P. MONCEAU, N. P. ONG, A. M. PORTIS, A. MEERSCHAUT, AND J. ROUXEL, *Phys. Rev. Lett.* **37**, 602 (1976).
10. J. CHAUSSY, P. HAEN, J. C. LASJAUNIAS, P. MONCEAU, G. WAYSAND, A. WAIN TAL, A. MEERSCHAUT, P. MOLINIE, AND J. ROUXEL, *Solid State Commun.* **20**, 759 (1976).
11. P. HAEN, F. LAPIERRE, P. MONCEAU, M. NUNEZ REGUEIRO, AND J. RICHARD, *Solid State Commun.* **26**, 725 (1978).
12. A. BEN SALEM, A. MEERSCHAUT, L. GUEMAS, AND J. ROUXEL, *Mater. Res. Bull.* **17**, 1071 (1982).
13. S. A. SUNSHINE AND J. A. IBERS, *Inorg. Chem.* **25**, 4355 (1986).
14. D. W. BULLETT, *J. Phys. C* **15**, 3069 (1982).
15. R. J. CAVA, F. J. DiSALVO, M. EIBSCHUTZ, AND J. V. WASZCZAK, *Phys. Rev. B* **27**, 7412 (1983).
16. T. E. PHILLIPS, R. P. SCARINGE, B. M. HOFFMAN, AND J. A. IBERS, *J. Amer. Chem. Soc.* **102**, 3435 (1980).
17. J. M. WATERS AND J. A. IBERS, *Inorg. Chem.* **16**, 3273 (1977).
18. P. J. SQUATTRITO, S. A. SUNSHINE, AND J. A. IBERS, *J. Solid State Chem.* **69**, 261 (1986).
19. D. A. KESZLER, J. A. IBERS, M. SHANG, AND J. LU, *J. Solid State Chem.* **57**, 68 (1985).
20. D. A. KESZLER AND J. A. IBERS, *J. Amer. Chem. Soc.* **107**, 8119 (1985).
21. A. BEN SALEM, A. MEERSCHAUT, H. SALVA, Z. Z. WANG, AND T. SAMBONGI, *J. Phys. (Orsay, Fr.)* **45**, 771 (1984).